

FATIGUE LIFE ASSESSMENT AND RELIABILITY ANALYSIS OF COPE-HOLE DETAILS IN STEEL BRIDGES

PING LIAO^{1,2*}, YONGBAO WANG³, XIUCHENG ZHANG¹,
RENDA ZHAO², YI JIA², HAIFENG ZHU¹

¹*School of Civil Engineering, Putian University, Putian Fujian, China*

²*School of Civil Engineering, Southwest Jiaotong University,
Chengdu Sichuan, China*

³*College of Civil Engineering, Taiyuan University of Technology,
Taiyuan Shanxi, China*

Received 30 April 2018; accepted 20 August 2019

Abstract. Cope-hole details are widely applied to steel bridges. However, the safety of steel bridges is influenced by the fatigue performance of welded details. So, cope-hole details with flange and web subjected to axial loads were selected as the research object. Based on the basic theory of linear elastic fracture mechanics and the Finite Element Method, the stress intensity factors of cope-holes details were calculated. The influences of geometry size and crack size of the detail on the stress intensity factors were then investigated. The Paris model of fatigue crack propagation predicted the crack propagation life of cope-hole details. Besides, the fatigue limit-state equation was also established to analyse the effect of random variables (such

* Corresponding author. E-mail: liaoping@ptu.edu.cn

Ping LIAO (ORCID ID 0000-0003-0850-0643)
Yongbao WANG (ORCID ID 0000-0002-7201-8846)
Xiucheng ZHANG (ORCID ID 0000-0002-9263-8612)
Renda ZHAO (ORCID ID 0000-0002-8251-4755)
Yi JIA (ORCID ID 0000-0001-9267-6021)
Haifeng ZHU (ORCID ID 0000-0002-6166-8835)

Copyright © 2020 The Author(s). Published by RTU Press

This is an Open Access article distributed under the terms of the Creative Commons Attribution License (<http://creativecommons.org/licenses/by/4.0/>), which permits unrestricted use, distribution, and reproduction in any medium, provided the original author and source are credited.

as initial crack size, critical crack size, crack propagation parameter) on the fatigue reliability index. Finally, the recommended value of the detection period was present. The results show that the stress intensity factor gradually increases with the increase of the cope-hole radius, the weld size, the flange plate thickness, the crack length and the web thickness. However, it gradually decreases with the increase of the ratio of the long and short axle to the crack. The predicted number of fatigue cyclic loading required by the fatigue crack depth propagating from 0.5 mm to 16 mm under nominal stress amplitude of 63 MPa is 122.22 million times. The fatigue reliability index decreases with the fatigue growth parameter, the crack shape ratio and the mean of initial crack size increasing, which is relatively sensitive. However, the variation coefficient of the initial crack size has little effect on it. The detection period of cope-hole details is the service time corresponding to the fatigue accumulated cyclic loading of 198.3 million times.

Keywords: detection period, fatigue crack propagation life, fatigue reliability index, fracture mechanics, stress intensity factors.

Introduction

The stress concentration phenomenon caused by multiple weld crossover is avoided effectively by using cope-hole details, which has been widely applied in steel bridges. This detail has been included in some valid design codes (*EN 1993-1-9 Eurocode 3. Design of Steel Structures – Part 1-9: Fatigue*; Hobbacher, 2008). With the increase of the service time of bridges, fatigue cracks appeared in many details of steel bridges. For the fatigue, scholars have carried out the problem of cope-hole details, as reported by the recent research, many types of research. The fatigue tests of the cope-hole details existing in the I-section beam bent in-planes were carried out. The fatigue strength and local stress were also investigated (Miki & Tateishi, 1997). Because of the local stress near the cope-hole, the fatigue strength of this detail was desperately low. Aygül, Al-Emrani, M., & Urushadze (2012) evaluated the application of hot spot stress method and effective notch stress method in welded joints with cut-out holes of the orthotropic steel bridge deck. If the welds were omitted, the hot spot stress calculated by the shell element model was distorted to be especially significant. The fatigue tests of cope-hole details with the flange and web subjected to axial loads were carried out, and the *S-N* curve of this detail was obtained (Liao, Wei, Xiao, & Tang, 2016; Wei, Xiao, & Pei, 2017). Choi, Tateishi, & Hanji (2013) discussed the effect of burr grinding on the fatigue strength of cope-hole details. The fatigue strength and nodal local stress behaviour of I-section beams with cope-hole details were also studied by fatigue tests. The results show that when cope-hole details were subjected to significant shear stress, the burr grinding

had little improvement on the fatigue strength. For cope-hole details in the orthotropic steel bridge deck, the fatigue crack initiation was predicted by critical distance theory (Zhou, Wen, Wang, Zhang, & Du, 2016). The initiation life of fatigue crack based on the critical distance theory and the *S-N* curve of raw materials was in good agreement with the fatigue test results. Inevitably, there are some initial defects in the manufacturing process of welded details, which causes local stress concentration and accelerate the fracture of structures.

Many scholars gradually adopted the fracture mechanics method to study the fatigue crack propagation of welded details with initial defect (Nagy, Wang, Culek, Van Bogaert, & De Backer, 2017). As an essential parameter in fracture mechanics, the stress intensity factor not only determines the crack growth of the welded details but also has a direct effect on the prediction accuracy of the fatigue life (Albuquerque, Silva, de Jesus, & Calçada, 2015; Duchaczek & Mańko, 2015). Many methods have been developed to solve stress intensity factors, such as analytical method, numerical method and experimental method. Jie (2015) adopted FRANC3D to model the cruciform welded details. Based on the basic theory of the linear elastic fracture mechanics, the influence of different corrosion pit size, crack shape and crack depth on the stress intensity factor of welding details were studied. Chung, Lin, R., & Lin, K. (2011) proposed a numerical and experimental method based on the least-squares method to investigate the mixed-mode stress intensity factors of cruciform welded details. The influence of different geometric parameters on the stress intensity factor was discussed. It was also verified by non-contact optical experiment. Zhao, Haldar, & Breen Jr (1994) took the butt-welded details of a steel box girder with the flange subjected to tensile loads as the research background. The fatigue limit-state equation was established by using the theory of the linear elastic fracture mechanics and the reliability theory. The fatigue reliability index of steel bridge members was also calculated. The analysis results show that the stress intensity factor was more sensitive to the crack size.

In this paper, the stress intensity factors of cope-hole details with flange and web under axial loads were first analysed by the numerical method. Parameter sensitivity analysis of the stress intensity factor was emphatically discussed. Then the fatigue life of this detail was predicted by using the Paris crack propagation model. Under the basic theory of the linear elastic fracture mechanics, the fatigue limit equation of welded details was constructed. The influence of random variables on fatigue reliability index was analysed. Finally, the recommended value of the inspection period for cope-hole details was presented.

1. Stress intensity factor and propagation life prediction

1.1. Stress intensity factor

One cope hole is generally installed to access the crossing welds at the intersection of weld lines (Choi, Tateishi, & Hanji, 2013). Cope-hole details often appear in orthotropic steel deck and splice members of steel bridges. Sometimes some initial defects, such as micro-cracks, inevitably exist at the weld toe. Stress intensity factor is an important physical parameter reflecting the strength of the stress field at the crack front, which determines whether or not the crack grows, and the rate of crack growth (Jie, 2015).

The stress intensity factors at the crack front are expressed as (Li, 2008):

$$K_i = \lim_{r \rightarrow 0} \sqrt{2\pi r} \sigma_{jk}(r, 0), \quad (1)$$

where i – the type of crack; r is the distance from the points to the crack front; $\sigma_{jk}(r, 0)$ is the stress of the points near the crack front.

For I-mode cracks, the following formula is used to calculate the stress intensity factor (Jie, 2015).

$$K_I = Y \sigma \sqrt{\pi a}, \quad (2)$$

where a – crack size, mm; Y – crack shape correction factor.

For mixed-mode cracks, when the point near the crack front satisfies $\frac{r}{a} \ll 1$, the asymptotic displacement field of three kinds of cracks using complex stress function are expressed as follows (ANSYS Inc, 2009):

$$u = \frac{K_I}{4\mu} \sqrt{\frac{r}{2\pi}} \left[(2k-1) \cos \frac{\theta}{2} - \cos \frac{3\theta}{2} \right] + \frac{K_{II}}{4\mu} \sqrt{\frac{r}{2\pi}} \left[(2k+3) \sin \frac{\theta}{2} + \sin \frac{3\theta}{2} \right], \quad (3)$$

$$v = \frac{K_I}{4\mu} \sqrt{\frac{r}{2\pi}} \left[(2k+1) \sin \frac{\theta}{2} - \sin \frac{3\theta}{2} \right] - \frac{K_{II}}{4\mu} \sqrt{\frac{r}{2\pi}} \left[(2k-2) \cos \frac{\theta}{2} + \cos \frac{3\theta}{2} \right], \quad (4)$$

$$w = \frac{K_I}{4\mu} \sqrt{\frac{r}{2\pi}} \sin \frac{\theta}{2}, \quad (5)$$

where r and θ represent the polar coordinates of the reference points near the crack front, mm and degree; u , v and w indicate the displacement of the reference point near the crack front in the local coordinate

system, mm; μ – the shear modulus, N/mm²; K_I , K_{II} and K_{III} are defined as the stress intensity factor of front crack points and for the plane strain problem – $k = 3 - 4\nu$, and plane stress problem – $k = \frac{3 - \nu}{1 + \nu}$.

The geometric parameters and crack information have a direct influence on the stress and displacement fields. The stress intensity factors are directly related to the geometric parameters and crack information of the structure. Geometric parameters mentioned in the Eqs (1)–(5) mainly refer to plate thickness, cope-hole radius and weld size. The crack information includes initial crack size, critical crack size and cracks propagation parameter.

1.2. Finite Element Model of three-dimensional fracture mechanics

1.2.1. Modelling details

The fatigue crack initiation and propagation diagram of the cope-hole detail with flange and web subjected to axial loads is given in Figure 1 (Liao, Wei, Xiao, & Tang, 2016). The geometric dimension of this detail is shown in Figure 2. Three-dimensional fracture mechanics model was established by ANSYS to analyse fatigue crack growth life and stress intensity factors of front crack points. In modelling, one surface semi-elliptical crack was introduced at the toe of butt weld between the web and the flange near the cope-hole. From the stress field and displacement field near the crack front, it was known that the stress near the crack front points tends to infinity, but the area has succumbed to be plastic status. Therefore, single elements are used to express the stress

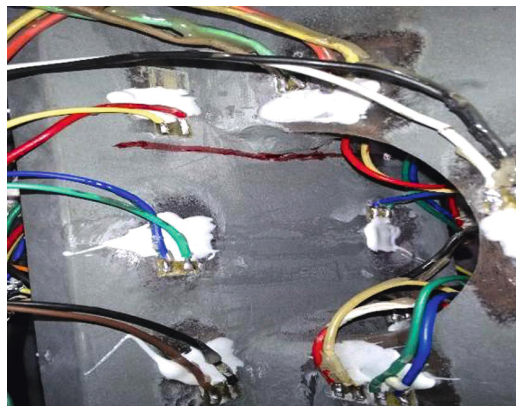


Figure 1. Crack propagation diagram

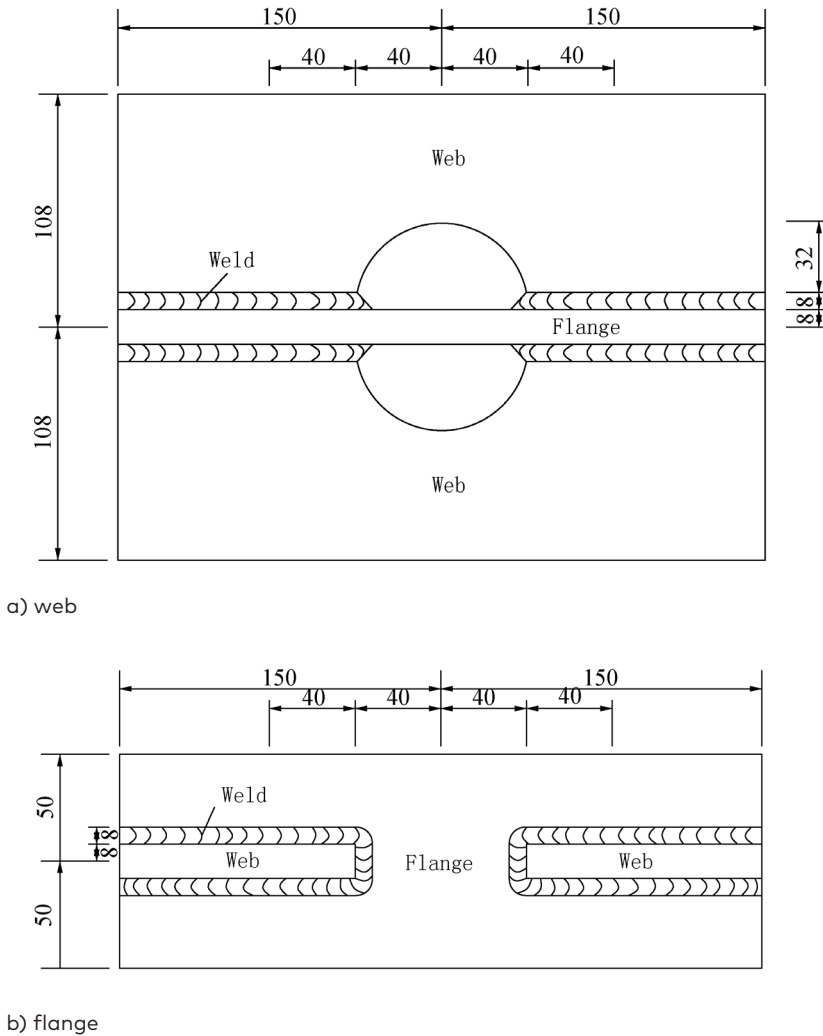
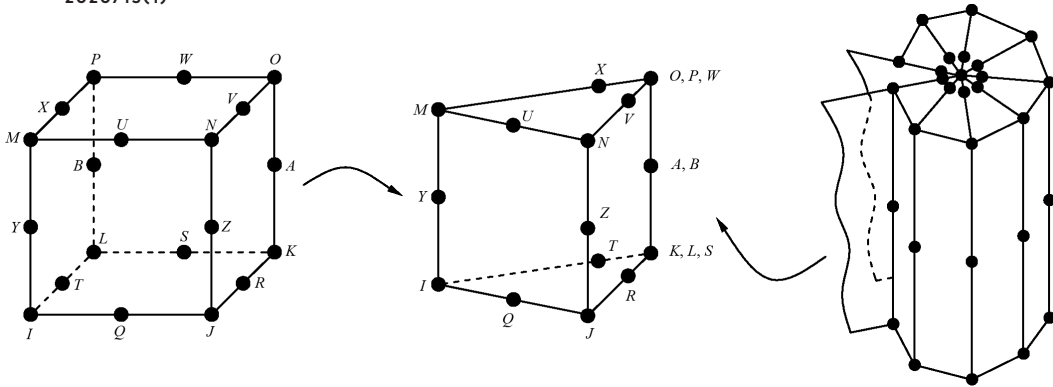


Figure 2. The geometry of the cope-hole details

singularity in calculation and analysis. For three-dimensional cracks, the stress singularity is considered by the three-dimensional one-quarter node singular element generated by the degradation of SOLID95 elements, as shown in Figure 3.

The calculation accuracy of the stress intensity factors is related to the singular element length, the crack depth and the number of elements around the crack front. Cao, Yang, Packer, & Burdekin (1998) suggested that the ratio of the singular element length to the crack



Note: units in mm.

Figure 3. A singular element of the three-dimensional crack model

depth be less than 0.1. Ingraffea & Manu (1980) considered that this ratio was between 0.05 and 0.15. However, the technical document of ANSYS software required that the ratio was less than 0.125. In this paper, this ratio was 0.1 when the stress intensity factor and its influence parameters were investigated. The second layer elements around the crack front were first set up by the SOLID45 element. Then, the first layer elements of non-singular SOLID45 surrounding the crack front were generated by adding the crack front nodes. The

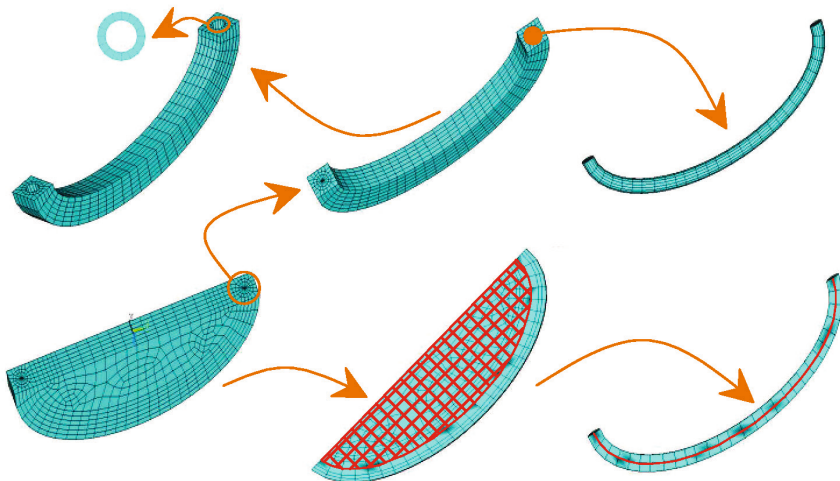


Figure 4. Three-dimensional Finite Element Model of the crack body

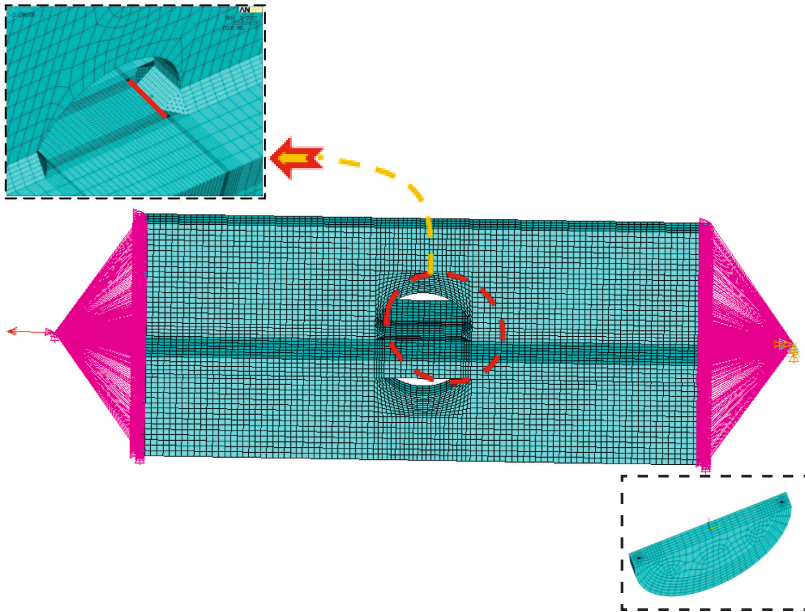


Figure 5. Three-dimensional Finite Element Model of fracture mechanics by ANSYS

first layer of non-singular elements was singularly processed through macro commands, and three-dimensional one-quarter node singular elements were generated. Finally, the other parts of cope-hole details were established. The three-dimensional view of the crack body was shown in Figure 4. The Finite Element Model (FEM) of three-dimensional fracture mechanics for cope-hole details was presented in Figure 5. Uniformly distributed tensile load of 70 MPa was applied at one end of the FEM, and a fixed constraint was applied at the other end. Static analysis and solution were carried out. Then the stress intensity factor of each node of the crack front was calculated by the one-quarter nodal displacement method.

1.2.2. The geometry of the Finite Element Model

The longitudinal length of the Finite Element Model (FEM) is 460 mm. The cope-hole radius r is 40 mm. The flange thickness y_{yb} and the web thickness fb are both 16 mm. The weld size hf is 8 mm. The width of the flange plate and semi-web is 100 mm and 200 mm, respectively. The length to short axis ratio n of the semi-elliptical crack is 2. The semi-crack length a is 12 mm.

1.2.3. Model verification

Based on the established three-dimensional fracture mechanics model, the stress intensity factor K_I of this welded detail is $14.64 \text{ MPa}\cdot\text{m}^{1/2}$ and the calculation result of Eq. (2) is $13.59 \text{ MPa}\cdot\text{m}^{1/2}$ (assuming that the crack shape correction factor $Y = 1$). The difference between the two results is 7.7%. It shows that the FEM is feasible to analyse the stress intensity factor, and its accuracy is acceptable. This model was used to investigate the influence factors of stress intensity factors and fatigue reliability index in the following.

1.3. Influencing factors of stress intensity factors

The stress and displacement fields of structures under loads depend on the geometric information of components. The stress intensity factors vary with different geometric sizes. The difference is directly related to the geometric parameters and crack information of the structure. Chung, Lin, R., & Lin, K. (2011) consider the impact of the geometric and crack parameters on mixed-mode stress intensity factors for load-carrying fillet welded cruciform joints using the least-squares method. Therefore, besides the influence of the singular element length, the crack depth and the number of elements around the crack front, the impact of the geometric and crack parameters of welded details on the stress intensity factor of the structure is also notable. The stress intensity factor is K_I . The angle described in each diagram is the angle between the flange plate surface and the line that is formed by connecting each node at the crack front and the ellipse centre, which is shown in Figure 6.

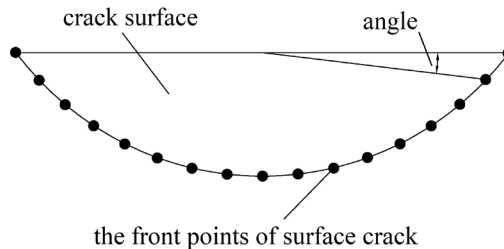


Figure 6. The angle between the front points of the surface and flange plate surface

1.3.1. Geometric parameter

In this section, the variation law of stress intensity factor with geometric parameters changing is discussed. When a parameter is analysed, the other geometric and crack parameters remain unchanged.

Table 1. Geometric parameters used in the Finite Element Model

Weld size, mm	Web thickness, mm	Flange thickness, mm	Cope-hole radius, mm
6	12	12	2.4
7	14	14	3.2
8	16	16	4.0
9	18	18	4.8
10	20	20	5.6

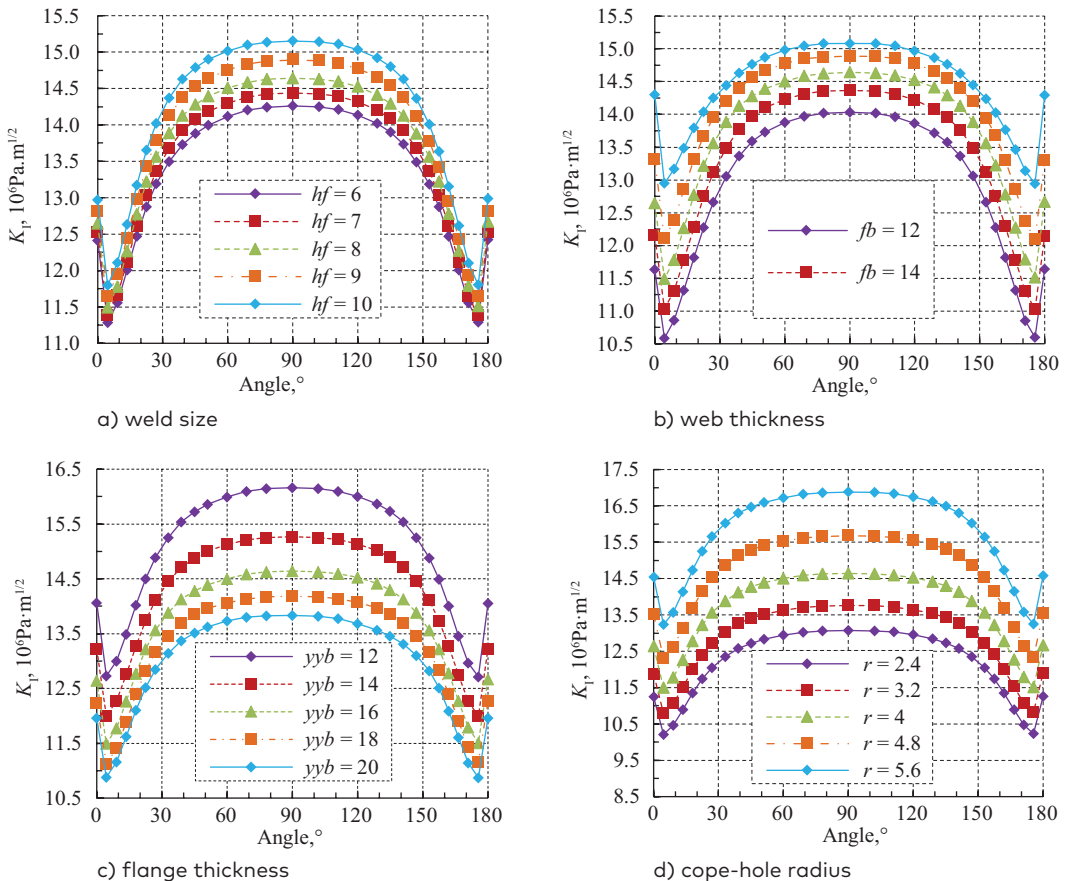


Figure 7. Stress intensity factor affected by different geometric parameters

Parameters used in the FEM are shown in Table 1. The calculation results of K_I versus different geometric parameters are presented in Figure 7.

Under Figure 7, the maximum value of K_I is approximately obtained at 90 degrees and the minimum value is obtained at 175.5 degrees. That is to say, K_I reaches the maximum value at the deepest point of the surface crack. There is the same distribution of K_I at the crack front when geometric parameters are changed in the FEM. Stress intensity factor at each node at the crack front gradually increases with increasing of weld size and the web thickness, as shown in Figure 7a. From Figure 7c, it is seen that the thinner the flange thickness, the lower the flange thickness. According to Figure 7d, K_I of each node at the crack front rapidly enlarges with the cope-hole radius increasing. The influence of the cope-hole radius on the stress intensity factor is bigger than that of other geometric factors.

2.3.2. Crack parameter

Cope-hole details have been discussed to evaluate the impact of crack parameters on the stress intensity factors. When a crack parameter is analysed, the other geometric parameters and crack parameters remain unchanged. Changed parameters used in the FEM are shown in Table 2. The calculation results of K_I influenced by crack length and length ratio between long and short axis are given in Figure 8.

From Figure 8, the maximum and minimum values obtain approximately at 90 degrees and 175.5 degrees, respectively. When the angle is less than 27 degree or more than 145 degrees, the crack length has little effect on the stress intensity factor. When n changes from 2 to 3, the minimum values of K_I is obtained at 175.5 degrees. If $n > 3$, the minimum value is obtained at 0 degree and 180 degrees. To some extent, the length to axial ratio changes the distribution of stress intensity factors of each point at the crack front. Stress intensity factor of each node at the crack front rises with the crack length increasing. The effect of crack length on K_I of these points near the deepest point of the surface, crack is bigger than that of other locations. It is notable that, with the increase of the length to short axis ratio, the stress intensity factor of each node at the crack front gradually decreases. The length to the axial ratio of semi-elliptical crack has a relatively less influence on the stress intensity factor near the deepest point of the surface crack.

Table 2. Crack parameters used in the Finite Element Model

Parameter type	Value				
The length to short axis ratio	2.0	2.5	3.0	3.5	4.0
The crack length/mm	10.0	11.0	12.0	13.0	14.0

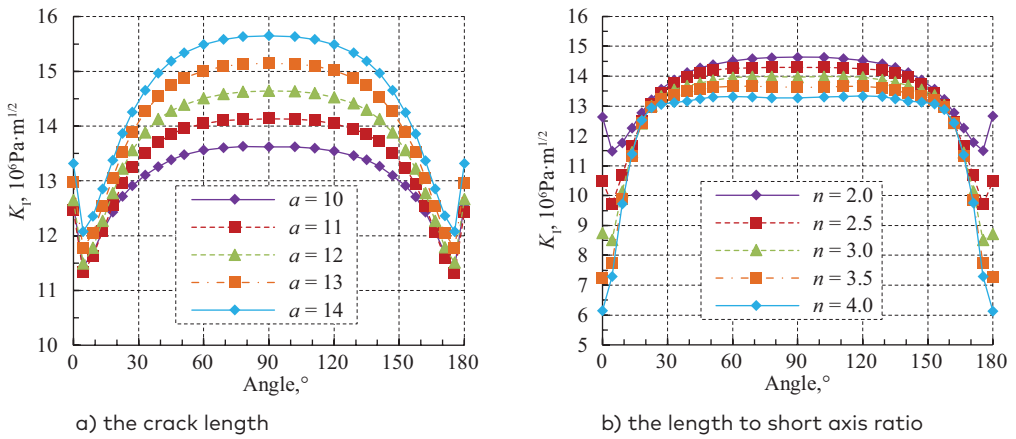


Figure 8. The relationship between stress intensity factor and crack parameters

2.4. The correction coefficient of crack shape

According to the stress intensity factors results of the crack front points when the length to short axis ratio was 2; they were shown in Table 3.

The cubic-polynomial correction coefficient function of crack shape $F(a)$ of the deepest point of the surface crack was fitted by the basic principle of the least square method and calculation results of crack shape coefficient Y according to the Eq. (2). The expression of $F(a)$ is presented below:

$$F(a) = -2.7732 \left(\frac{a}{t} \right)^3 + 7.5630 \left(\frac{a}{t} \right)^2 - 5.5226 \left(\frac{a}{t} \right) + 2.7012, \quad (6)$$

where a represents the crack size, mm; t indicates the flange thickness ($t = ybb$).

Table 3. The stress intensity factors of the crack front points ($n = 2$)

Semi-crack length, mm K_I	$K_{I, 106Pa \cdot m^{1/2}}$
10.00	13.62
11.00	14.13
12.00	14.64
13.00	15.15
14.00	15.65

2.5. Propagation life prediction of fatigue crack

According to the Paris crack propagation model, it is known that:

$$\frac{da}{dN} = C \cdot (\Delta K)^m, \quad (7)$$

$$\Delta K = Y \sigma \sqrt{\pi a}, \quad (8)$$

$$\int_{a_0}^{a_c} \frac{da}{C(Y \cdot \sqrt{\pi a})^m} = (\Delta \sigma)^m, \quad (9)$$

where a_c – critical crack size or upper limit of crack length; a_0 indicates the initial crack size or lower limit of crack length; ΔK – stress intensity factor amplitude; $\Delta \sigma$ – defined as stress amplitude; C and m are both material constants; N represents fatigue cyclic loading times.

The formula of fatigue crack growth rate of steel in the air or non-harsh environment was given, in which $m = 3.0$ and $C = 5.21 \cdot 10^{-13}$ (*BS 7910:2013 Guide to Method for Assessing the Acceptability of Flaws in Metallic Structures*). Jie (2015) gave the material parameter of fatigue crack propagation m and C for cruciform welded details with no corrosion pits, and the inclined angle of 0 degrees, which were equal to 3.0 and $1.676 \cdot 10^{-13}$, respectively. Cope-hole details investigated in this paper were close to those of Jie (2015) in terms of stress state, geometrical structure and crack propagation path. These parameters provided by Jie (2015) were used to predict the propagation life of fatigue crack for this cope-hole detail.

Under Eqs. (6) and (9), when the fatigue crack depth propagates from 0.5 mm to 16 mm under nominal stress amplitude of 63 MPa, the predicted number of fatigue load is 122.22 million times.

3. Fatigue reliability analysis of cope-hole details

3.1. Fatigue limit state equation

The stress intensity factor under the equivalent stress amplitude is expressed as

$$\Delta K = F(a) \sigma_{eq} \sqrt{\pi a}, \quad (10)$$

where σ_{eq} – the equivalent stress amplitude applied to the welded details; $F(a)$ – the fatigue crack shape coefficient function of the welded details.

The Eq. (10) is substituted into the Eq. (7), and the following formula is obtained by a simple transformation.

$$\frac{da}{(F(a)\sqrt{\pi a})^m} = (\sigma_{eq})^m C dN. \quad (11)$$

By integrating the two sides of Eq. (11), the following formula is obtained:

$$\int_{a_0}^{a_c} \frac{da}{(F(a)\sqrt{\pi a})^m} = (\sigma_{eq})^m C (N_c - N_0), \quad (12)$$

where a_0 , a_c denote the initial and critical crack size, respectively; N_0 , N_c are the cumulative stress cycles corresponding to a_0 and a_c , respectively.

The critical fatigue cumulative damage to welded details is defined as follows:

$$H(a_0, a_c) = \int_{a_0}^{a_c} \frac{da}{(F(a)\sqrt{\pi a})^m}. \quad (13)$$

Therefore, the fatigue limits state Eq. (14) based on the fatigue reliability method of the linear elastic fracture mechanics is established by Eq. (12) and Eq. (13). Its expression is as follows:

$$g(X) = \int_{a_0}^{a_c} \frac{da}{(F(a)\sqrt{\pi a})^m} - (\sigma_{eq})^m C (N_c - N_0). \quad (14)$$

3.2. Random variable analysis

3.2.1. Initial crack size a_0

The distribution of initial crack size is determined by non-destructive evaluation and equivalent initial flaw size method. A large number of research results show that the fatigue life of welded details is very sensitive to the initial crack size. Zhang & Mahadevan (2001) pointed out that the initial fatigue crack obeyed logarithmic normal distribution. The mean values were in the range of 0.1 mm~2.5 mm. The variation coefficient was 0.08~0.60. When the fatigue reliability index of the welded details was analysed in this paper, the initial crack size was assumed to be a logarithmic normal distribution with the mean of 0.5~1.5 mm and the variation coefficient of 0.20~0.60.

3.2.2. Critical crack size a_c

When the fracture toughness of the material is doubled, the critical crack size calculated by the fracture mechanics criterion increases by three times. However, fatigue life only increases by 5%. Therefore, the critical crack size has little effect on the fatigue life of welded details (Li, 2008). As stated in Zhao (1995), the critical crack size of welded details was taken as the thickness or width of the welded details. Therefore, in this paper, the critical crack size was taken as 16 mm when analysing the fatigue reliability of welded details.

3.2.3. Crack propagation parameters

Because of the distribution characteristics of fatigue crack-propagation parameters, many scholars have done many types of research. It is considered that the fatigue crack-propagation parameter m is a constant. The fatigue crack-propagation parameter C obeys the lognormal distribution. Its variation coefficient is within the range of 0.1~0.6 (Liu & Mahadevan, 2009; Zhang & Mahadevan, 2001; Zhao, 1995; Zhao, Haldar, & Breen Jr, 1994). Zhao, Haldar, & Breen Jr (1994) thought that C obeyed logarithmic normal distribution. Its mean and variation coefficient are $6.89 \cdot 10^{-12}$ and 0.63, respectively. The fatigue crack-propagation-parameter C is $5.739 \cdot 10^{-14}$ when analysing the fatigue reliability index of the upper chord members and the crossbeams of steel bridge (Li, 2008). Li (2003) obtained the fatigue crack-propagation parameter C of scrap steel of a railway steel bridge by the fatigue test, which was $5.15 \cdot 10^{-10}$ when the stress ratio was 0.1. Therefore, the fatigue crack-propagation parameter C has obvious uncertainty. It was assumed that the fatigue crack-propagation parameter $m = 3$ and the fatigue crack-propagation parameter C obeyed logarithmic normal distribution when analysing the fatigue reliability of welded details. Its mean and variation coefficient are $3.5 \cdot 10^{-10} \sim 6.9 \cdot 10^{-10}$ m/cycle/(MPa·m^{1/2})^m, 0.4~0.6, respectively.

3.3. Parameter analysis of fatigue reliability index

The parameters selected for fatigue reliability analysis are shown in Table 4.

Taylor Series expands the structural performance function at the corresponding point $P^*(x_1^*, x_2^*, \dots, x_n^*)$ of the utmost possible failure probability. The limit state equation is expressed as follows (Li, 2003):

$$Z \approx g(x_1^*, x_2^*, \dots, x_n^*) + \sum_{i=1}^n \frac{\partial g}{\partial x_i} \Big|_{P^*} (\mu_{x_i} - x_i^*) = 0. \quad (15)$$

Table 4. Parameters of fatigue reliability index

Parameters	Property	Mean	Variation coefficient
Equivalent stress amplitude	constant	70 MPa	0
Initial crack size a_0 , mm	variable, lognormal distribution	0.5-1.5	0.2-0.6
Critical crack size a_c , mm	constant	16	0
Fatigue crack-propagation parameter C	variable, lognormal distribution	$(3.5-6.9) \cdot 10^{-10}$	0.4-0.6
Fatigue crack-propagation parameter m	constant	3	0

As stated in the Eq. (15), the mean and variance of Z are obtained. The reliable index of the structure is expressed as:

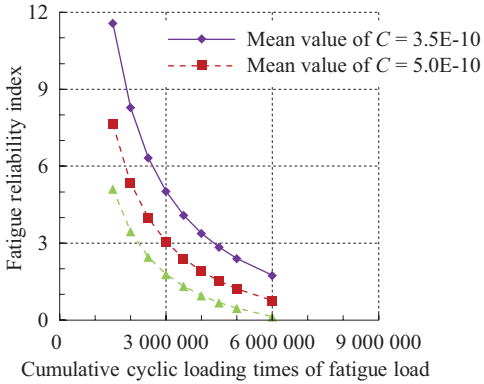
$$\beta = \frac{\mu_Z}{\sigma_Z} = \frac{Z \approx g(x_1^*, x_2^*, \dots, x_n^*) + \sum_{i=1}^n \frac{\partial g}{\partial x_i} \Big|_{P^*} (\mu_{x_i} - x_i^*)}{\left[\sum_{i=1}^n \left(\frac{\partial g}{\partial x_i} \Big|_{P^*} \sigma_{x_i} \right)^2 \right]^{0.5}}. \quad (16)$$

After the non-normal variables are transformed into the standard normal ones, the fatigue reliability index of the welded details with the cope-hole is calculated by the iterative method. The influence of random variables on fatigue reliability index of welded details is illustrated in the section taking this cope-hole detail as an example.

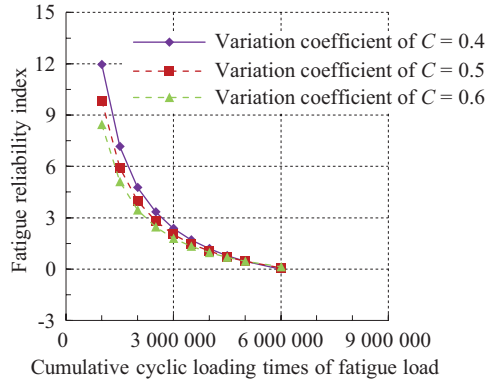
The initial values of random variables are as follows: The initial crack size and coefficient variations are 1 mm and 0.2, respectively. The

Table 5. Discrete values of random variables

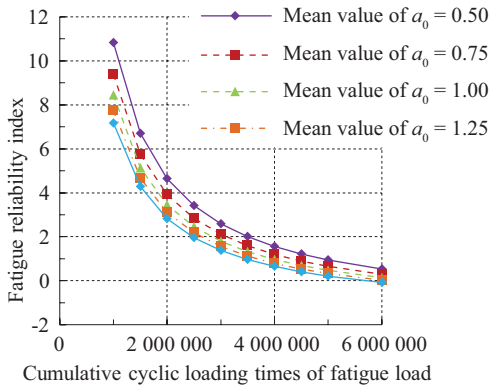
Initial crack size a_0 , mm		Fatigue crack-propagation parameter, C		Crack shape ratio, n
Mean value	The variation coefficient	Mean value	The variation coefficient	value
0.50	0.2	$3.5 \cdot 10^{-10}$	0.2	2
0.75	0.3	$5.0 \cdot 10^{-10}$	0.3	3
1.00	0.4	$6.9 \cdot 10^{-10}$	0.4	4
1.25	0.5	-	0.5	-
1.50	0.6	-	0.6	-



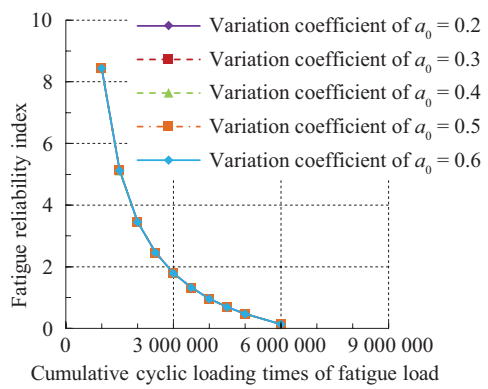
a) mean value of C



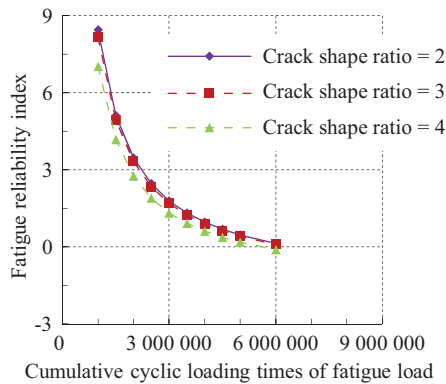
b) variation coefficient of C



c) mean value of a_0



d) coefficient variation of a_0



e) crack shape ratio

Figure 9. Fatigue reliability index under different random variables

variation coefficient of $C = 0.6$ and its mean value is $6.9 \cdot 10^{-10}$ m/cycle/ $(\text{MPa} \cdot \text{m}^{1/2})^m$. The crack shape ratio $n = 2$. When a variable is analysed, the other variable and parameters remain unchanged. Discrete values of random variables used in the FEM are presented in Table 5. The calculation results of fatigue reliability index versus different variables are presented in Figure 9.

As shown in Figure. 9, the fatigue reliability index rapidly decreases with the increase of the cumulative loading times of fatigue load. With the mean value of C , the variation coefficient of C , mean value of a_0 , moreover, crack shape ratio n increasing, the fatigue reliability index gradually decreases, and the effect was significant. However, fatigue reliability index only changes to a small extent with the increase of the coefficient variation of a .

3.4. Inspection period

During the operation process of welded details, the higher the reliability index of the specified fatigue target is, the higher the structure safety is. The corresponding maintenance inspection period is shortened. The required maintenance cost also markedly increases. The fatigue reliability index of each structural detail of supported steel plate beams is 2.31~7.28. The β_{target} of railway steel bridge is 3.0 or 3.5. The European Steel Association recommended that the β_{target} of all steel bridges be 3.5. In this paper, the β_{target} of the welded detail with cope-holes was taken as 3.5. The fatigue reliability index of welded details after maintenance and reinforcement was assumed to be the same as the original fatigue reliability index. Based on the fatigue reliability

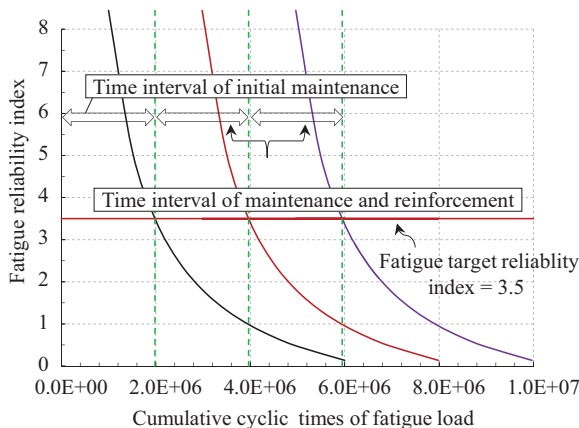


Figure 10. Inspection period

index results of section 3.3, the formulated inspection period is shown in Figure 10.

When the cumulative cyclic loading times of fatigue load reach 198.3 million times, the fatigue reliability index of the cope-hole details reduced to 3.5. Only after the maintenance and reinforcement meet the corresponding requirements, it continued to be put into operation.

Conclusions

In this study, the stress intensity factors, fatigue life evaluation and fatigue reliability analysis of cope-hole details were investigated by the fracture mechanics and numerical method. The conclusions are as follows:

1. The stress intensity factor gradually increases with the increase of the cope-hole radius, the weld size, the flange plate thickness, the semi-crack length and the web thickness. However, it gradually decreases with the ratio of the long and short axle to the crack ascending.
2. When the fatigue crack depth propagates from 0.5 mm to 16 mm under nominal stress amplitude of 63 MPa, the predicted number of fatigue load is 122.22 million times.
3. The fatigue reliability index decreases with fatigue growth parameter, crack shape ratio and the mean of initial crack size increasing, which is relatively sensitive. However, the variation coefficient of the initial crack size has little effect on it. The detection period of cope-hole details is the service time corresponding to the fatigue accumulated cyclic loading times of 198.3 million.

Acknowledgement

This research was supported by the scientific subsidisation project for the talented person of Putian University (2018075), the Natural Science Foundation of Fujian (2016J01253) and China railway corporation research and development of science and technology key project (2013G001-A-2).

REFERENCES

- Albuquerque, C., Silva, A. L., de Jesus, A. M., & Calçada, R. (2015). An efficient methodology for fatigue damage assessment of bridge details using modal superposition of stress intensity factors. *International Journal of Fatigue*, *81*, 61-77. <https://doi.org/10.1016/j.ijfatigue.2015.07.002>
- ANSYS Inc (2009). *Release 12.0 documentation for ANSYS*. Research Report. USA: ANSYS Incorporated.
- Aygül, M., Al-Emrani, M., & Urushadze, S. (2012). Modelling and fatigue life assessment of orthotropic bridge deck details using FEM. *International Journal of Fatigue*, *40*, 129-142. <https://doi.org/10.1016/j.ijfatigue.2011.12.015>
- BS 7910:2013 *Guide to Method for Assessing the Acceptability of Flaws in Metallic Structures*
- Cao, J. J., Yang, G. J., Packer, J. A., & Burdekin, F. M. (1998). Crack modeling in FE analysis of circular tubular joints. *Engineering Fracture Mechanics*, *61*(5-6), 537-553. [https://doi.org/10.1016/S0013-7944\(98\)00091-5](https://doi.org/10.1016/S0013-7944(98)00091-5)
- Choi, S. M., Tateishi, K., & Hanji, T. (2013). Fatigue strength improvement of weld joints with cope hole. *International Journal of Steel Structures*, *13*(4), 683-690. <https://doi.org/10.1007/s13296-013-4009-7>
- Chung, H. Y., Lin, R. S., & Lin, K. J. (2011). Evaluations of mixed-mode stress intensity factors for load-carrying fillet welded cruciform joints using the least-squares method. *Journal of the Chinese Institute of Engineers*, *34*(2), 265-285. <https://doi.org/10.1080/02533839.2011.565598>
- Duchaczek, A., & Mańko, Z. (2015). Determination of the value of stress intensity factor in fatigue life of steel military bridges. *European Journal of Environmental and Civil Engineering*, *19*(8), 1015-1032. <https://doi.org/10.1080/19648189.2014.992549>
- EN 1993-1-9 *Eurocode 3. Design of Steel Structures – Part 1- 9: Fatigue*
- Hobbacher, A (2008). Recommendations for fatigue design of welded joints and components. IIW document IIW – 1823-07, ex XIII – 2151 r4 – 07/XV – 1254r4-07.
- Ingraffea, A. R., & Manu, C. (1980). Stress-intensity factor computation in three dimensions with quarter-point elements. *International Journal for Numerical Methods in Engineering*, *15*(10), 1427-1445. <https://doi.org/10.1002/nme.1620151002>
- Jie, Z. Y. (2015). Study on the fatigue performance of welded joints in steel bridges under prior corrosion and complex stress fields (Doctoral dissertation, Dissertation, Southwest Jiaotong University (in Chinese))
- Li, Y. (2008). *Research on fatigue performance and reliability of highway steel bridges*: (Doctoral dissertation, Dissertation, Harbin Institute of Technology, Harbin, (in Chinese))
- Li, Z. (2003). An Expression of Fatigue Crack Propagation Velocity with Reliability, *Journal of Xi'an Petroleum Institute (Natural Science Edition)* *18*(6): 67-70. (in Chinese)

- Liao, P., Wei, X., Xiao, L., & Tang, J. S. (2016). Experimental study on the girder's new detail fatigue performance of Hutong Railway Yangtze River Bridge. *China Civil Engineering Journal*, (8), 9. (in Chinese)
- Liu, Y., & Mahadevan, S. (2009). Probabilistic fatigue life prediction using an equivalent initial flaw size distribution. *International Journal of Fatigue*, 31(3), 476-487. <https://doi.org/10.1016/j.ijfatigue.2008.06.005>
- Miki, C., & Tateishi, K. (1997). Fatigue strength of cope hole details in steel bridges. *International Journal of Fatigue*, 19(6), 445-455. [https://doi.org/10.1016/S0142-1123\(97\)85727-1](https://doi.org/10.1016/S0142-1123(97)85727-1)
- Nagy, W., Wang, B., Culek, B., Van Bogaert, P., & De Backer, H. (2017). Development of a fatigue experiment for the stiffener-to-deck plate connection in Orthotropic Steel Decks. *International Journal of Steel Structures*, 17(4), 1353-1364. <https://doi.org/10.1007/s13296-017-1207-8>
- Wei, X., Xiao, L., & Pei, S. (2017). Fatigue assessment and stress analysis of cope-hole details in welded joints of steel truss bridge. *International Journal of Fatigue*, 100, 136-147. <https://doi.org/10.1016/j.ijfatigue.2017.03.032>
- Zhang, R., & Mahadevan, S. (2001). Reliability-based reassessment of corrosion fatigue life. *Structural Safety*, 23(1), 77-91. [https://doi.org/10.1016/S0167-4730\(01\)00002-9](https://doi.org/10.1016/S0167-4730(01)00002-9)
- Zhao, Z. (1995). Primary and deformation-induced high and low cycle fatigue reliability of infrastructure with updating through non-destructive inspection. (Doctoral dissertation, Dissertation, the University of Arizona, Tucson, Arizona)
- Zhao, Z., Haldar, A., & Breen Jr, F. L. (1994). Fatigue-reliability evaluation of steel bridges. *Journal of Structural Engineering*, 120(5), 1608-1623. [https://doi.org/10.1061/\(ASCE\)0733-9445\(1994\)120:5\(1608\)](https://doi.org/10.1061/(ASCE)0733-9445(1994)120:5(1608))
- Zhou, H., Wen, J., Wang, Z., Zhang, Y., & Du, X. (2016). Fatigue crack initiation prediction of cope hole details in orthotropic steel deck using the theory of critical distances. *Fatigue & Fracture of Engineering Materials & Structures*, 39(9), 1051-1066. <https://doi.org/10.1111/ffe.12402>